Proceedings World Geothermal Congress 2020+1
Reykjavik, Iceland, April - October 2021

A New Leapfrog Model and Geothermal Reservoir Model of Waesano, Indonesia

Ando Deuhart[1] and John O'Sullivan[1]

[1] Department of Engineering Science, The University of Auckland, Private Bas 90210, Auckland, New Zealand

adeu318@aucklanduni.ac.nz, jp.osulllivan@auckland.ac.nz

Keywords: 3D Geological Model, Geothermal Reservoir Model, Natural State Simulation, Waesano.

ABSTRACT

Waesano field is a high terrain geothermal system situated in West Manggarai Regency, East Nusa Tenggara, Indonesia. The heat source is believed to come from volcanic activity beneath a large caldera lake in the centre of the Waesano Caldera. Geothermometers from nearby hot springs give a reservoir temperature of 230ºC, with an associated power potential of 36 MWe. A comprehensive reservoir modelling study of Waesano geothermal area was carried out during this project in order to represent the subsurface condition of the system. Geology, geochemical and geophysics data from the Ministry of Energy and Mineral Resources of the Republic of Indonesia were used as inputs to the conceptual model of Waesano geothermal system that was developed. The conceptual model was then used to build a new 3D geological model using Leapfrog Geothermal and a new natural state reservoir model was set up using the AUTOUGH2 simulator. A good match to natural-state conditions was obtained by adjusting values of permeability and heat and mass inputs. The model was calibrated by comparing the model output to field data such as the locations of hot springs and temperature gradient information from two shallow wells. The new combined 3D geological model/reservoir model provides a valuable tool for supporting decision making aimed at ensuring the sustainable development and management of the system. It will also help with communication and engagement with the local community.

1. INTRODUCTION

Abundant geothermal resources have been discovered in Indonesia due to its location within the Ring of Fire of volcanic zone. Approximately 28,910 GW of geothermal energy potential have been identified from 312 locations. Currently, the utilisation ratio of the total potential is less than 5%. Future development of geothermal power plants is being aggressively targeted by the Indonesian Government. The government has issued new laws such as Law No.21 of 2014 which no longer classifies geothermal power generation as a mining operation to encourage geothermal development (Pambudi, 2018). Of all the potential resources, thirty-three were found across the Bali-Nusa Tenggara region, with a total energy potential of approximately 1872 MWe. Flores Island, located in Bali-Nusa Tenggara, has been declared a geothermal island by the Indonesian Government. Waesano geothermal field, on Flores Island, is a geothermal prospect from which it is planned to generate electricity soon (Figure 1A). Other notable geothermal prospects lie on the island (Figure 1B), including Oka-Kawalawu, Sokoria, Mataloko, Nage, Ulumbu, and Sembalun (Hochstein, 2010). However, few of these prospects have been developed. In fact Ulumbu and Mataloko are the only geothermal fields on which power plants have been constructed, with capacities of 10 MW and 2.5 MW respectively (Pambudi, 2018).

The concession area of Waesano is not within a conservation area or protected forest, and has an estimated power potential of 36 MWe (Direktorat Panas Bumi, 2017). There is no published 3D geological model or reservoir model which can be used to identify the characteristics and behaviour of the field. However, several studies have been published such as a geological survey, laboratory analyses, and geochemical and geophysical measurements. The geological survey was performed using the volcano-stratigraphy principle (Hadi, Kusnadi, & Simarmata, 2015). The surface manifestations are mostly hot springs with chloride and sulphate-chloride water with a geothermometer temperature of up to 230˚C. Laboratory analysis has also been conducted to investigate the petrography and rock alteration. Geophysical measurements such as geomagnetic strength, gravity, and magnetotelluric measurements were carried out. Two shallow exploration wells have also been drilled to measure the temperature gradient. These data are considered to be adequate for building an appropriate geological model and a preliminary natural state reservoir model of Waesano geothermal field.

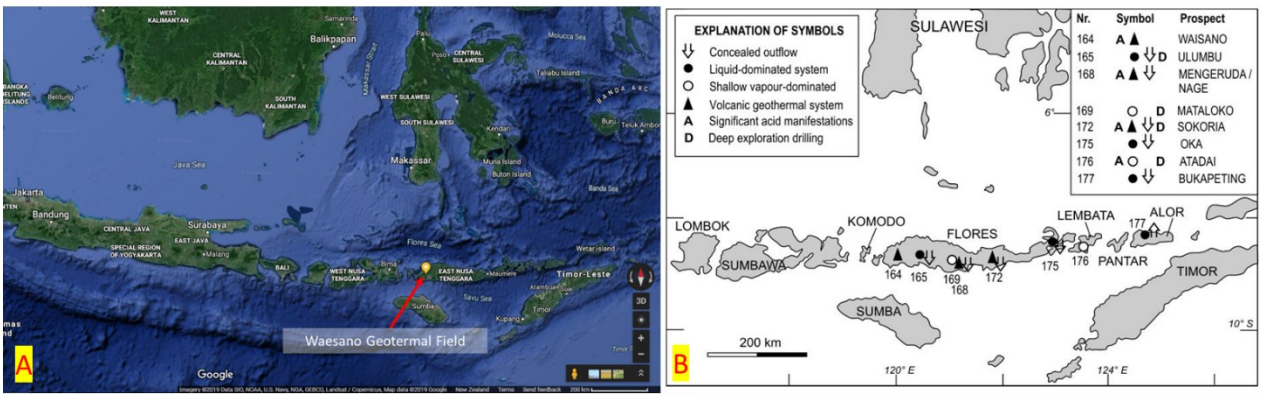

Figure 1: A. Location of Waesano geothermal field in East Nusa Tenggara (from Google, 2019) B. Various geothermal prospects within the magmatic Banda Arc (Hochstein, 2010)

2. GEOLOGICAL SETTING

Waesano geothermal system originated in the Tertiary period of the Miocene-Pliocene era, when a basin was formed into which sandstone sediment was deposited (Hadi et al., 2015). This sediment is found in the northwest around Labuan Bajo and in the northeast around Watuwangka (Figure 2). Tectonic activity created a northwest and southeast strike-slip fault which forms the basement structure, creating the rhyolite-dacite volcanic rock formation. A large eruption created the Beliling caldera, which is associated with ignimbrite products. Volcanism continues around Golo Kempo, Golo Tantong, Golo Leleng, and Golo Tanadereng, which are all composed of partially silicified basaltic rock. In the Pliocene era, volcanism at Poco Dedeng in the south produced dacite lava with a pyroclastic flow that spread over to Lembor. The northern part of Poco Dedeng was later covered due to the commencement of volcanism at Sano Nggoang, where there is a crater lake with acidic water.

2.1 Structural Geology

The analysis presented here is based on field observations and supported by lineaments from the Landsat image and Digital Elevation Mode (DEM) Map. The structures were classified as volcanic structures such as caldera and crater formations or faults. Volcanic structures are visible at the Beliling volcanic depression, the ellipsoid Sano Nggoang crater, and the semi-circular structure at Golo Leleng and Waemunting. The craters are thought to be the products of explosive acidic eruptions, especially Sano Nggoang which is filled with acid water. In the field steep circular crater walls can be observed. There have been at least three major eruptions which produced sulphur deposits and hot springs in the south-eastern part of Lake Sano Nggoang. The eruptions produced pyroclastic flows which spread to the north and southwest of the lake, where they were blocked by older volcanic products from Poco Dedeng (Hadi et al., 2015)

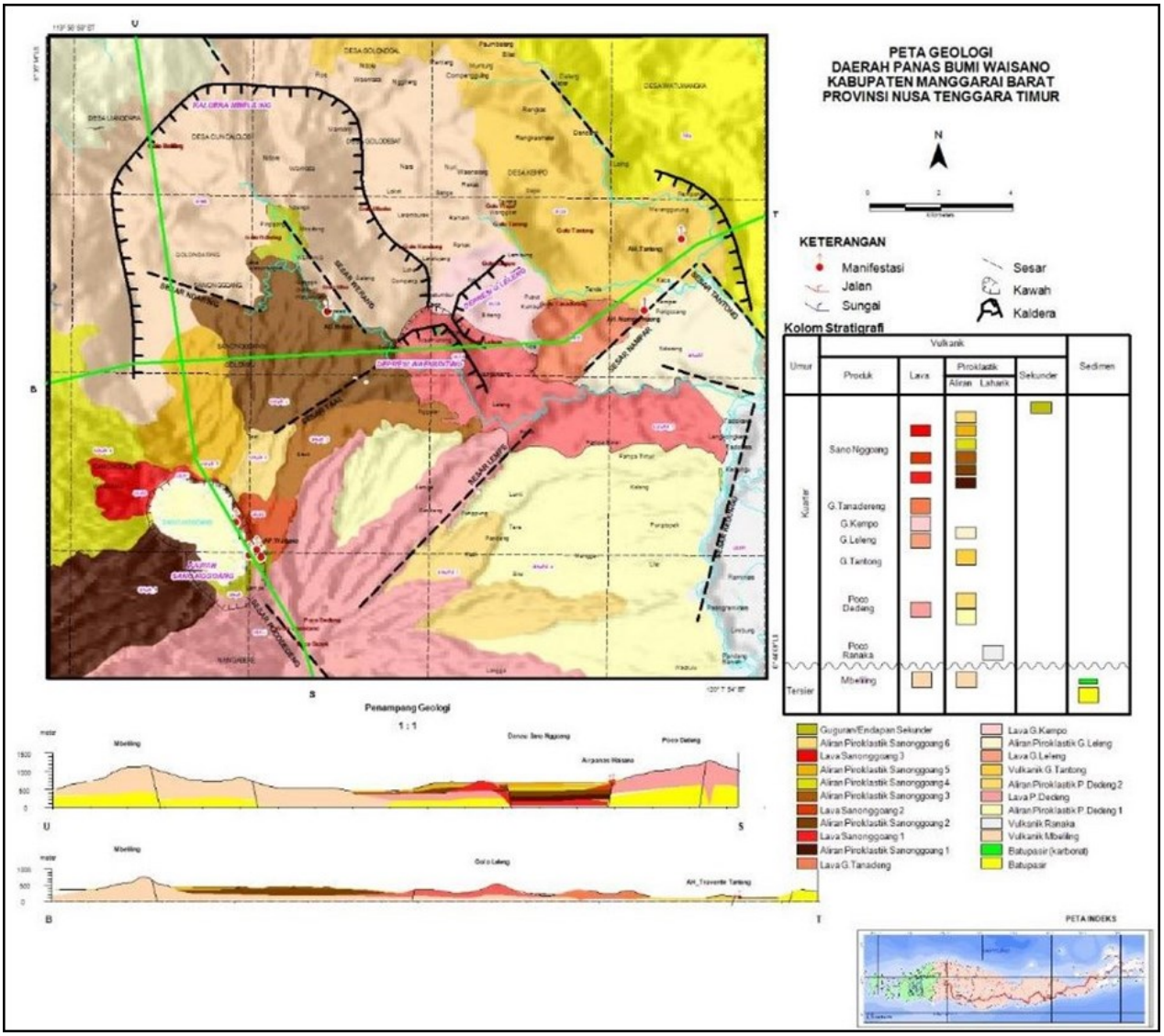

Figure 2: Geological map of Waesano geothermal system (Hadi et al., 2015)

2.2 Stratigraphy

Geological mapping divides each rock unit according to volcano-stratigraphy principles (Hadi et al., 2015). They are classified from the oldest rock to the youngest, following the dating of eruption products: Sandstone unit, Beliling Volcanic Unit, Ranaka Volcanic Unit, Poco Dedeng Volcanic Unit, Golo Tantong Volcanic Unit, Golo Leleng Volcanic Unit, Golo Kempo Volcanic Unit, Golo Tanadereng Volcanic Unit, and Sano Nggoang Volcanic Unit.

3. GEOCHEMICAL STUDIES

Most of the Waesano hot springs are located at the edge of Lake Sano Nggoang. However, Waesano hot spring 3 (APWS3) occurs 300 meters to the southeast of the lake. All hot springs appear clear and smell of sulphur. Silica sinters are deposited in APWS1, APWS2, and APWS4. The water sample from Lake Sano Nggoang, identified as ADS1, has a low pH at 2.52. It is believed that fumaroles occur somewhere within the lake (Hadi et al., 2015). Nampar Mancing warm spring (AHN) is located in the Sano Nggoang district, approximately 13 km to the northeast of Lake Sano Nggoang. Golo Lara warm spring (AHG) is located in the Beliling district, approximately 15 km to the northeast of Lake Sano Nggoang and 2 km to the northeast of AHN. All warm springs appear clear without any smell of sulphur. Travertine is found deposited in these two warm springs. However, it is uncertain whether both warm springs are related to Waesano geothermal system (Johnstone, 2005).

3.1 Ternary Diagram Analysis

Based on a Cl-SO_4-HCO_3 diagram the hot spring and lake water belong to the chloride and sulphate-chloride type, which suggests a reliable deep-water source (Figure 3A). According to a Na-K-Mg diagram, APWS1, APWS2, AHG, and AHN are located in the partial equilibrium zone (Figure 3B). Other manifestations indicate an immature water source, influenced by surface water. Based on a Cl-Li-B diagram, all water samples indicate that hot water interacts with the volcanic system (Figure 3C). The possibility of contamination by sediment rock must be considered for both Na-K-Mg and Ci-Li-B diagram.

Isotope plots of δD vs $\delta^{18}O$ indicate the neutral cold springs at Sapo, Bobo, Lolos 1, and Lolos 2 are located along the Meteoric Water Line (Figure 3D). APWS1 and APWS2 show, however, that they come from the deep-water source, and dilution with meteoric water is minor. However, as with the Na-K-Mg diagram and the Cl-Li-B diagram, the possibility of contamination from sediment rock needs to be considered. The fumarole is thought to be inside Lake Sano Nggoang as is indicated by the presence of acid water, although the temperature is low. At the edge of the lake, a neutral hot spring was found with a strong H_2S smell, a hissing sound, and bubbles of gas present. The dominance of CO_2 and N_2 in the bubbles of gas does not reflect magmatic volatiles.

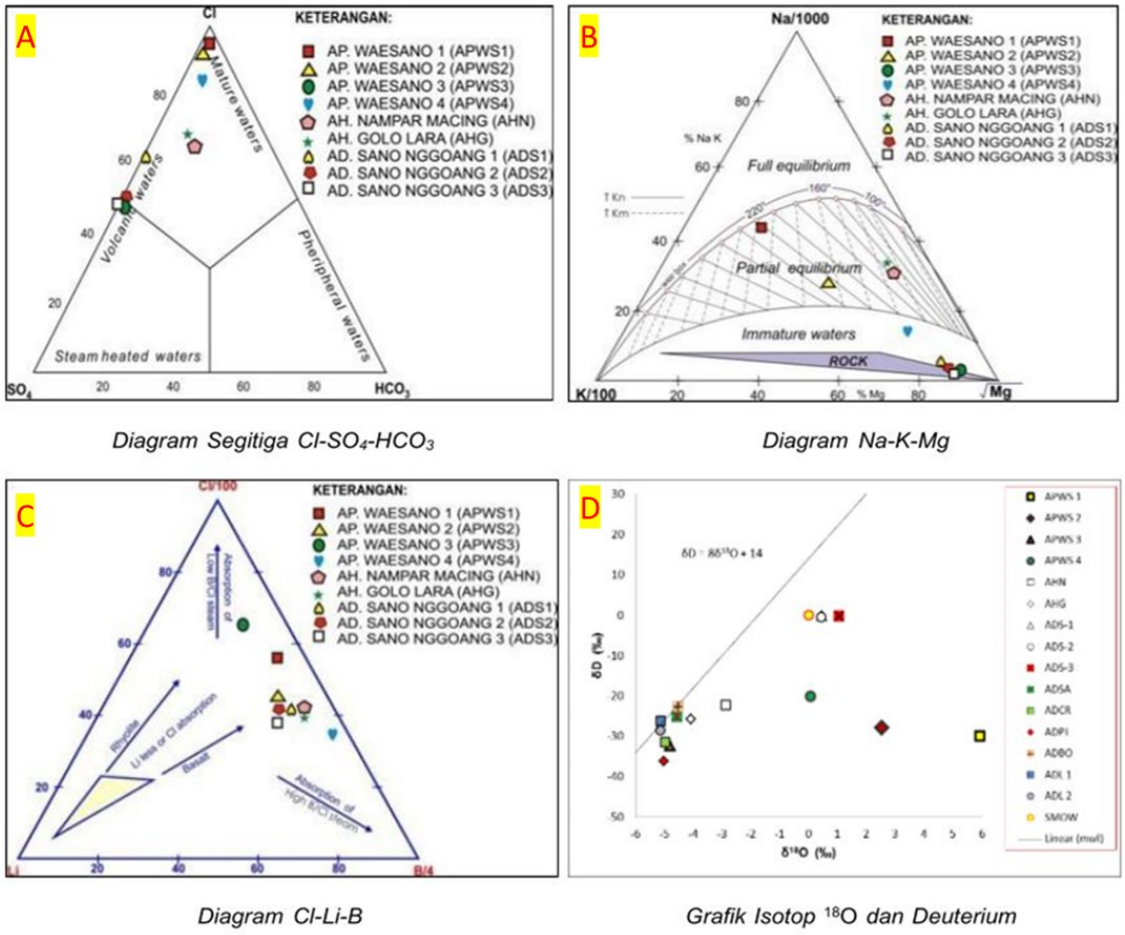

Figure 3: Geochemistry of Waesano Manifestations (Hadi et al., 2015)

The geothermal manifestations at Waesano are acid cold springs and neutral hot springs. They occur in a mixture of volcanic and sedimentary rocks which results in temperature variations and different chemical characteristics. The gas composition, from bubbles of gas obtained from APWS1, does not reflect the existence of a fumarole. The estimated temperature is only 150˚C based on a gas geothermometer. Based on the chemical composition of APWS2, it is possible to deduce the deep temperature. The SiO2 geothermometer indicates a low temperature of 150˚C. However, Na/K and Na/Li geothermometers indicate a high temperature of 273˚C and a moderate temperature of 193˚C, respectively. Based on all three geothermometers, the average temperature in the Waesano area is approximately 200˚C (Hadi et al., 2015).

4. GEOPHYSICAL SURVEYS

Geophysical measurements are necessary for geothermal exploration and complement the geological survey and geochemical analysis. There are three types of geophysical data which are published by the Indonesian Government, namely: gravitational, audio-magnetotelluric, magnetotelluric and time-domain electromagnetic (Kholid, Takodama, & Nurdin, 2015; Kholid & Widodo, 2015)

4.1 Gravity Method

The gravity method is corrected by the tide, tool drift, and standard gravity value to obtain the Bouguer Anomaly. Generally, the high and low anomalies appear in the north and the south, respectively, related to the fact that the volcanic products in the north are older than in the south. The lowest density of 2.3 gram/cm^3, is expected for young volcanic products such as lava and pyroclastic flow. A higher density of 2.68 gram/cm^3 is expected for the old volcanic products. The bottom formation has a density of 2.9 gram/cm^3, and is presumed to be basement sedimentary rock (Kholid et al., 2015)

4.2 Audio Magnetotelluric Method (AMT)

The resistivities are shown at 250, 500, 750, 1000, and 1500 m depths respectively (Figure 4). In the zone from 250 m to 500 m, the resistivity is <20 Ohm-m. It spreads to the north, east, west, and southeast. Low resistivity in the north, west, and east is associated with one elongated uniform pattern of lava and pyroclastic volcanic products, whereas in the southeast the resistivity is related to hydrothermal alteration. Meanwhile, moderate resistivity spreads to the northwest and northeast, associated with older volcanic products (Kholid et al., 2015).

The zone from 750 m to 1500 m, is dominated by low resistivity which has the same pattern at all depths. It occurs from the centre to the south with an inter-tonguing pattern to the northeast and is open to the southwest. With increasing depth, the resistivity becomes smaller to the southwest. 2D modelling shows the low resistivity <20 Ohm-m is related to the cap rock of Waesano geothermal system. It surrounds Lake Sano Nggoang as a result of Sano Nggoang volcanic activity to the southeast. The heat source is expected to be inside the active volcano, associated with the magmatic chamber of the eruption centre beneath Lake Sano Nggoang.

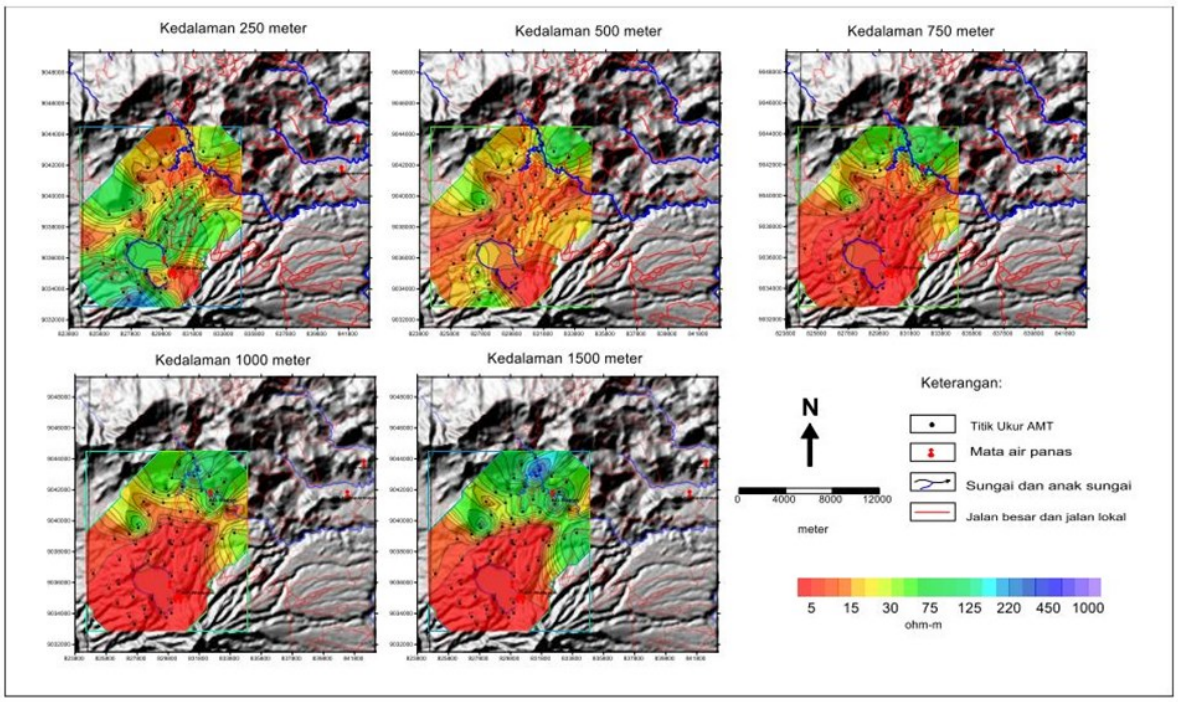

Figure 4: AMT resistivity of Waesano geothermal system (Kholid et al., 2015)

4.3 Magnetotelluric and Time Domain Electromeagnetic Method (MT-TDEM)

MT-TDEM was performed using a low frequency value of around 300-0,001 Hz. It measures resistivity at depths of 500 m, 1000, 1500 m, 2000 m, and 2500 m (Kholid & Widodo, 2015). This method can reach deeper than AMT, but with less accuracy. At 2000 m and 2500 m, the MT-TDEM data show an exciting resistivity pattern with a medium resistivity area surrounded by a low resistivity area. It shows that the cap rock is located to the southeast of Lake Sano Nggoang. The medium resistivity area which opens to the southeast is interpreted as the basement. 2D MT modelling shows that low resistivity (<20 Ohm-m) is expected to be the cap rock where hydrothermal alteration has taken place. On the other hand, the medium resistivity (20-200 Ohm-m) zone is thought to be the reservoir. Waesano hot springs arise from the gap between the existing structures from the reservoir at 1500 m.

5. WELL TEMPERATURE AND PRESSURE DATA

Well WW1: According to Nanlohi and Boegis (2003), the temperature at 250 m was measured at 46°C (Table 1). The temperature gradient is approximately 15.2°C per 100 metres. It was not considered high enough when compared to the average geothermal gradient (3°C/100m) to indicate a hot geothermal system. According to the Horner Plot method, the extrapolated temperature could reach 53°C. The Horner Plot method calculates the formation temperature after infinite time. It represents the actual formation

temperature, rather than the logging temperature which is measured after drilling. Pressure logging shows a maximum pressure of approximately 18 bars at 250 m. It was measured from the normal hydrostatic pressure from the drilling fluid and shows the water level is around 70 – 80 m below the surface.

Well WW2: According to Pusat Sumber Daya Geologi (2003), the temperature at 250 m was measured at 42˚C (Table 1). The temperature gradient is approximately 11.1˚C per 100 metres. The Horner Plot method shows that the extrapolated temperature could reach 52˚C. Meanwhile, pressure logging shows a maximum pressure of 12 bars at 250 m. This results in an estimated water level of at around 110 m depth.

Table 1: Available well data in WW1 and WW2

Information	Well	
	WW1	WW2
Depth	250 m	250 m
Location	119 59'48" E	120 00' 30" E
	08 41' 42" S	08 41' 18" S
Pressure Logging	18 bars	12 bars
Temperature Logging	46 ˚C	42˚C
Thermal Gradient	15.2˚C/100m	11.1˚C/100m
Horner Plot Temperature	53˚C	52˚C

6. CONCEPTUAL MODEL

Waesano geothermal system is related to the Quaternary volcanic system which is buried within the Sano Nggoang crater (Hadi et al., 2015) . The crater elevation reaches 700 masl, which means it is a high terrain volcanic system. The volcano is still active, shown by the acid lake water, hot springs, sulphurous smell, sulphur deposits, and rock leaching due to acid fluid. Fluid and magmatic volatiles of H_2S and CO_2 rise due to buoyancy effects and mix with H_2O to become acid water (Figure 5). Meteoric water infiltrates the Podo Dedeng slope, Sano Nggoang, and Beliling surface from above the ground. It forms a deep aquifer which is trapped inside sedimentary rock around Sano Nggoang to form the reservoir. This fluid is mixed with the magmatic fluid, and based on isotope traces, it shifts to the right side of the meteoric water line (MWL). The resulting chloride fluid is then trapped by the impermeable caprock on top of the reservoir. In Waesano, this caprock is dominated by clay types such as montmorillonite, kaolinite, alunite, and illite to the southeast of Lake Sano Nggoang.

The heat source is the main component of the geothermal system. The magmatic chamber is expected to be below Lake Sano Nggoang, being the eruption centre of the active volcanic system. Based on Fission Track method results, Sano Nggoang lava was created 0,2 ± 0,1 million years ago, during the Holocene period. Chemical analysis indicates high SO_2 levels in the southeast of the lake around the manifestations. This confirms that the heat source comes from the active volcano inside Sano Nggoang crater. The base of the reservoir, which is predicted to be carbonate sandstone, cannot yet be determined.

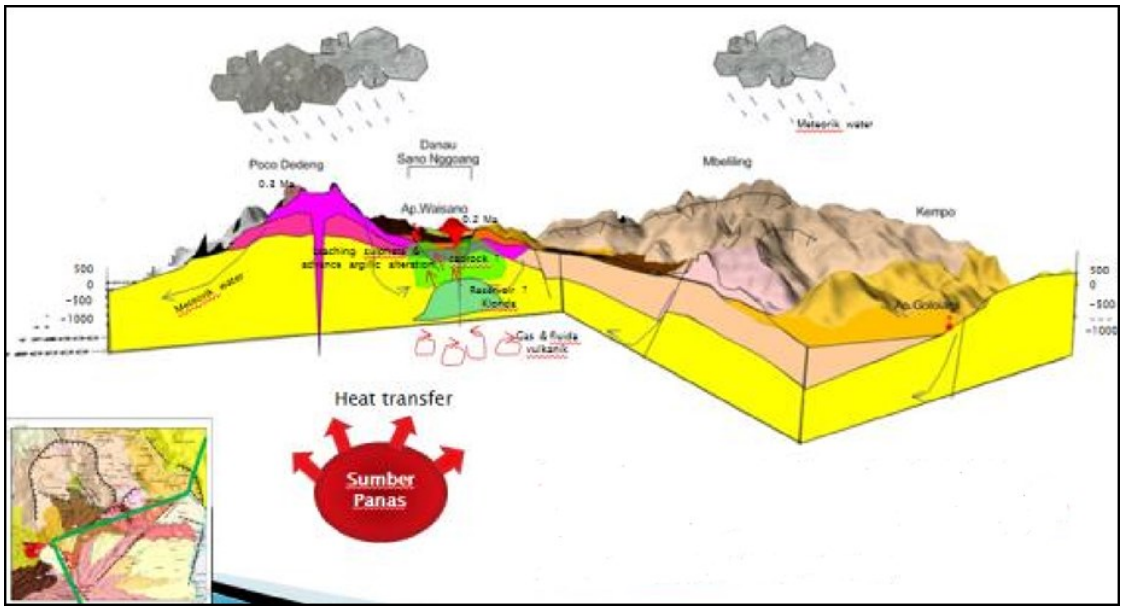

Figure 5: Conceptual model of Waesano geothermal system (Hadi et al., 2015)

7. 3D GEOLOGICAL MODEL CONSTRUCTION

The geological model was constructed using Leapfrog Geothermal, a 3D software package developed by Seequent. All of the following available data from the literature review is required, including: topography, well data, geological maps, cross-sections, and geophysical measurements.

7.1 Topographical Setup

The design of this geological model covers an area of 1600 km^2 (40 km x 40 km). Lake Sano Nggoang is located approximately in the centre of the map. The topography file was initially in latitude and longitude decimal format. After converting this to UTM format, the generated XYZ data were inserted into Leapfrog (Figure 6).

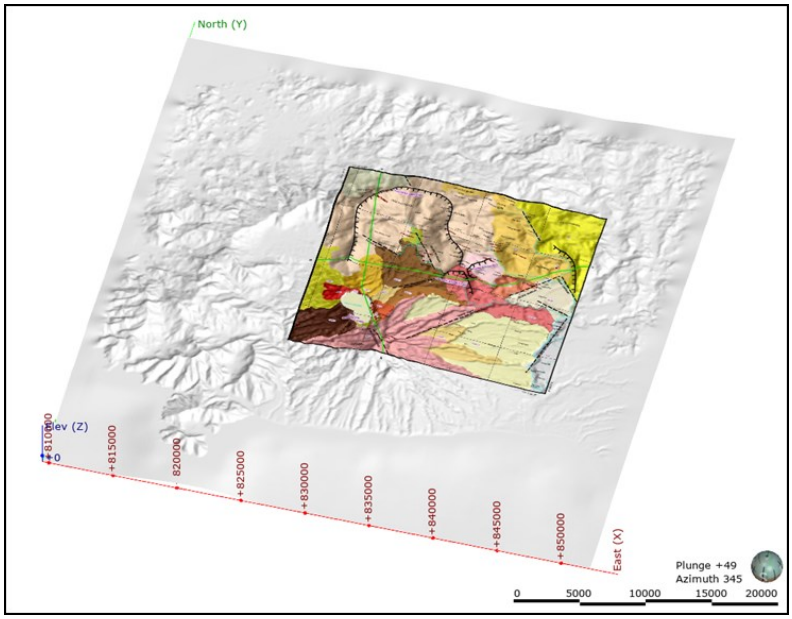

Figure 6: The geological map overlaid on top of the topography in Leapfrog

7.2 Stratigraphic Setup

The most comprehensive geological map of Waesano geothermal field is shown, as inserted in the exact X and Y location (Figure 6). Available cross-sectional information from the geological map was also inserted along with geophysical measurements. Those data are used as the primary sources in creating the stratigraphy. Based on the geological information, the rock units were classified into smaller groups, thus simplifying the geological model generation. The classifications are based on the geologic age of each rock unit. As a result, the Waesano rock formation was divided into six groups, which are Young Volcanic, Upper Quaternary Volcanic, Mid Quaternary Volcanic, Lower Quaternary Volcanic, Sedimentary, and Basement. The basement formation is included as a formation that is deeper than the sedimentary rocks. Table 2 summarises the Waesano rock stratigraphy.

Table 2: Summary of rock stratigraphy at Waesano

Rock Unit	Geologic Age
Sandstone	Sedimentary
Beliling	Tertiary Volcanic
Poco Ranaka	Lower Quaternary Volcanic
Poco Dedeng	Lower Quaternary Volcanic
Golo Tantong	Mid Quaternary Volcanic
Golo Leleng	Mid Quaternary Volcanic
Golo Kempo	Upper Quaternary Volcanic
Golo Tanadereng	Upper Quaternary Volcanic
Sano Nggoang	Young Volcanic

The available well data are from only two shallow exploration wells, with depths of 250 m. Inserting "artificial wells" manually helps with the interpretation of the lithology for the entire area (Figure 7A). Each artificial well was positioned from the surface down to an elevation of 3000 mbsl. The lithology for each well was assigned manually based on the geological map and regional geological maps. Two regional maps were also used (1:250,000 scale) in this study, Komodo and Ruteng, and smaller regional maps (1:50,000 scale) with higher resolution: Gili Motang, Kenari, Nangalili, and Werang (Badan Geologi, 2019).

7.3 Structural Set-up

Fault and caldera structures were created from the geological map. They were digitised using the polyline function on Leapfrog. The dip of the faults ranged from vertical to 75° based on the cross-section map. These structures separate the model into smaller output volumes which behave as small geological models. All these blocks are combined into one geological model that covers the lithology of the entire area (Figure 7B).

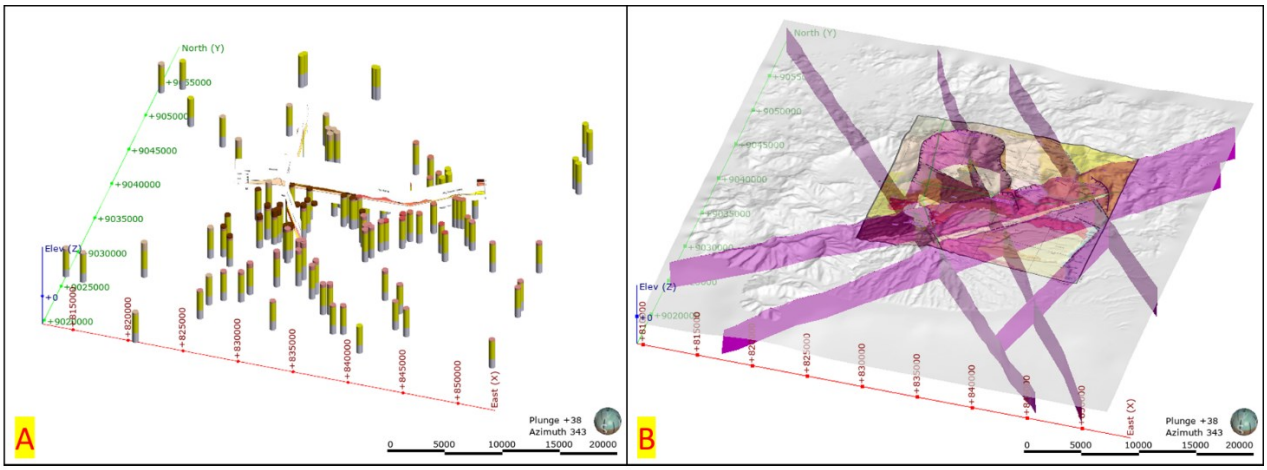

Figure 7: A. Cross section showing artificial wells in Leapfrog, B. Structures generated in Leapfrog

7.4 Alteration Setup

Resistivity from both the AMT and MT-TDEM data was used to create the alteration model. The polylines are drawn manually based on the resistivity map at each depth. AMT results at 250 m, 500 m, 750 m, 1000 m, and 1500 m and AMT-TDEM results at 2000 m and 2500 m were used to create the polyline (Figure 8). The resistivity boundary in this model is set at 20 ohm-m (Kholid et al., 2015). The alteration model will define the altered and unaltered rocks. Altered rock will be considered as the caprock of the geothermal system in the reservoir model.

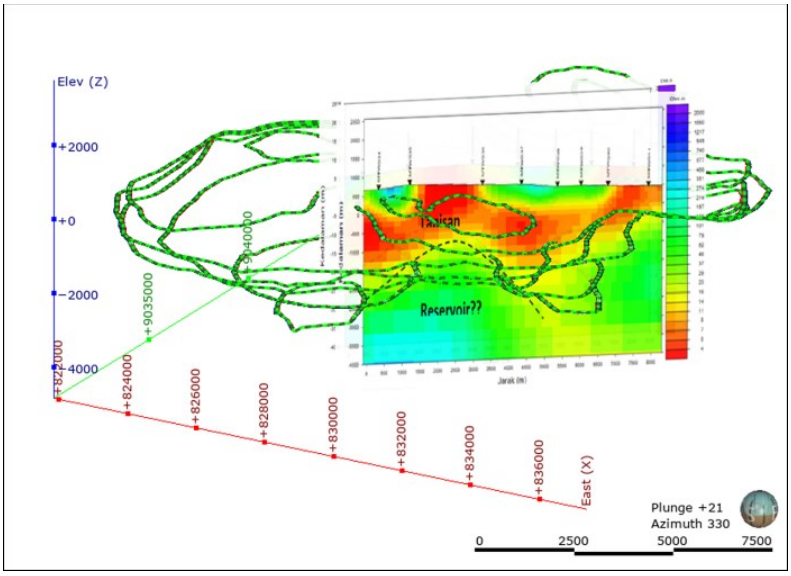

Figure 8: Alteration Polyline in Leapfrog

8. 3D GEOLOGICAL MODEL

Initially, the geological model is created after assigning the lithology and using the structural model to create smaller output volumes of fault blocks. In addition to the artificial wells, manual calibration is also needed to determine the lithology contacts in the subsurface down to 3000 mbsl using the polyline and structural disk functions in Leapfrog.

8.1 Geological Model

Seven faults and one caldera are assigned in the model. Seventeen blocks were made based on the structures. All of these blocks were combined into one large block covering 40 x 40 km. In total, seven lithologies were generated in the geological model from the oldest to the youngest which are Basement, Sedimentary, Lower Quaternary Volcanic, Mid Quaternary Volcanic, Upper Quaternary Volcanic, and Young Volcanic (Figure 9A).

8.2 Alteration Model

Some polyline adjustments were required outside the resistivity map. The final alteration model was created after some manual calibration, giving a reasonable caprock system (Figure 9B). There are two defined rock-types in this alteration model, namely: altered rock and unaltered rock.

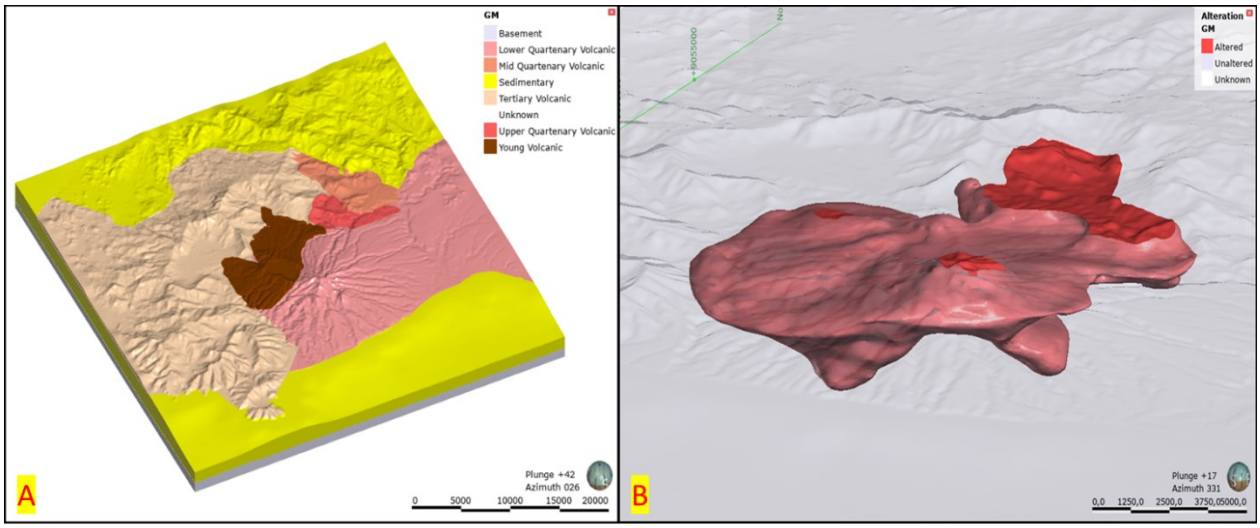

Figure 9: A. Geological model of Waesano in Leapfrog, B. Alteration model of Waesano in Leapfrog

9. NUMERICAL MODEL DEVELOPMENT

9.1 Reservoir Model Grid Setup

The geometry file covers the specific area of interest for Waesano geothermal system (Figure 10). The centre of the grid is around Lake Sano Nggoang where upflow is thought to be beneath the lake. The resistivity boundary is also located around the lake. The grid extends to the northeast to include the expected outflow of the geothermal system. This tentative outflow is located more than 10 km to the northeast of Lake Sano Nggoang. The side boundary of the system extends to the coastline in the south. The grid designed for this study covers an area of 334.08 km^2 (14.4 km in NW-SE direction, and 23.2 km in NE-SW direction). Around Lake Sano Nggoang, the grid blocks are smaller than at the edges. The smaller grid blocks will provide higher resolution in the numerical model in representing the hydrothermal flow.

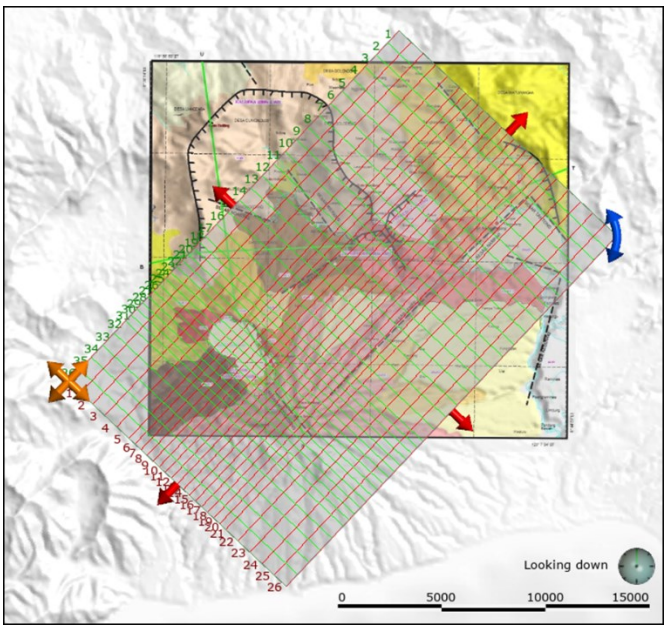

Figure 10: Grid Setup in Leapfrog

The size of the grid blocks ranges from 800m x 800m to 400m x 400m. The grid consists of 33 layers, with the thickest layer being 500m and the thinnest layer 100m. The number of elements or blocks is 20,920. Rectangular blocks are used in the model. The orientation of the grid is dominantly NE-SW, rotated from the north to the east by around 43.3°. Hence, it aligns the grid with NE-SW faults which are assumed to be the major faults within the geothermal system. This orientation will assist in adjusting the model parameters such as making one horizontal permeability higher than the other. The top of the model follows the topography from 50-1250 masl, whereas the bottom of the model is set at 3000 mbsl. The thickness of the layers is not constant, with the thicker layers being placed at the base, and the thinner layers being assigned to the top of the model.

The geological model grid is established in Leapfrog. The grid blocks are assigned the lithology from the geological model, including the fault and caldera structures. Consequently, every fault intersection in a certain lithology will have its own rock type. Every fault in the geological map contributes to building the grid. By applying a similar method, the alteration model grid can be generated. The alteration model grid dimensions and azimuth must have the same values as the geological model grid.

The generated geological and alteration model grid was then combined and optimized using the PyTOUGH scripting library (Figure 11). The scripting process also included other tasks, such as: A. Correcting the rock type and structure (e.g. fault, caldera) names; B. Setting the boundary conditions in the AUTOUGH2 model; C. Creating surface rock types with greater permeability for rainfall infiltration; D. Adding rainfall values and atmospheric pressure; E. Adjusting the lake depth. Initially, the lake was not included in the geological model. Later, it was added to the geometry file. According to Indonesia-tourism.com (2019), the depth of the lake is approximately 600 m. This data was used although there has not been an actual bathymetrical survey. The deepest point is assumed to be in the centre of the lake.

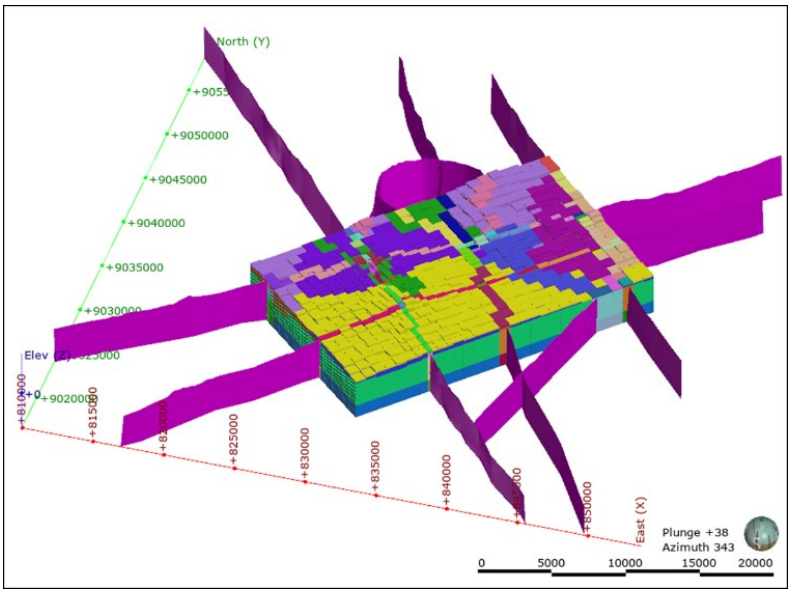

Figure 11: Reservoir model grid layout in Leapfrog

9.2 Boundary Condition

Top Boundary: Atmospheric conditions applied at the surface of the blocks are set at one bar pressure, a mean annual temperature of 21.8°C and annual rainfall of 2832 mm/year (Climate-data.org, 2019). An infiltration rate of 10% was set for rainfall in the Waesano area. This rainfall is input as an inflow of cold water into the top surface of the model with an enthalpy of 83.9 kJ/kg (20°C). The EOS3 equation of state (water, air) was utilised in this model to allow the simulation of a flow of a mixture of water and air, thus enabling the model to include the vadose zone near the surface. Therefore, water vapour and air in the gas phase contribute their partial pressures: Pg = Pa + Pv (Pruess et al., 1998).

Side Boundary: There is no heat or mass coming into or out of the system, thus it is assumed there are no-flow boundary conditions at the side boundaries. In the model set up the side boundaries may not be far enough to the southwest, in contrast to the northeast. The relatively close location of the boundary may affect the flow direction.

Base boundary: A conductive heat flux of 80mW/m^2 is assigned to the whole system. Waesano geothermal system is assumed to be a liquid-dominated reservoir. Therefore, mass inflows are put into the base of the model (Layer 33) at several points around the potential hot area. For the calibration process, the locations for the upflows are adjusted.

10. NATURAL STATE SIMULATION

In this natural state model, a total time of 1E+16 seconds or about 3.17E+8 years is assigned for reaching steady state condition. The method used for model set-up was to distribute the deep mass flow in more than one location. Some deep mass flows were injected in the Poco Dedeng Fault, which is strongly believed to be the main permeability control. Other mass flows were assigned to the Lempe and Nampar Faults, which are also strongly believed to be the permeability control for the outflow in the Tantong area.

11. MODEL OUTPUTS AND CALIBRATION

The calibration of the model was carried out using a manual process. Some data sets can be used as the baseline/benchmark for manual calibration, such as surface heat loss, chloride chemistry, or pressure and temperature profiles from the wells. The calibration process only involved two shallow exploration wells at Waesano. The quantity of mass flow was also calibrated to manage the heat input. The enthalpy was adjusted to manage the high temperatures near the bottom layer.

New rock-types and faults were introduced inside the reservoir. The faults within the caprock were also adjusted to have higher permeability. While the surrounding cap rock is close to impermeable, the faults are believed to have high permeability. The faults act as permeability controls to allow the fluid to rise to the surface, especially where there are hot spring manifestations near Lake Sano Nggoang. The permeability was then adjusted for the rock-types and faults, both outside and inside the reservoir. Generally, the

permeability outside the reservoir was reduced while inside the reservoir it was increased. As well as the vertical permeability, the lateral permeability was also adjusted. The natural state simulation results were calibrated with the following observed data:

Temperature and pressure well data: Satisfactory results were gained for matching the shallow temperature and pressure from the existing well (Figures 12). From the simulation, the temperature reaches approximately 220˚C and 245˚C respectively at 3000 mbsl (Figure 12A). Meanwhile, pressure in both wells was expected to reach about 300 bars (Figure 12B).

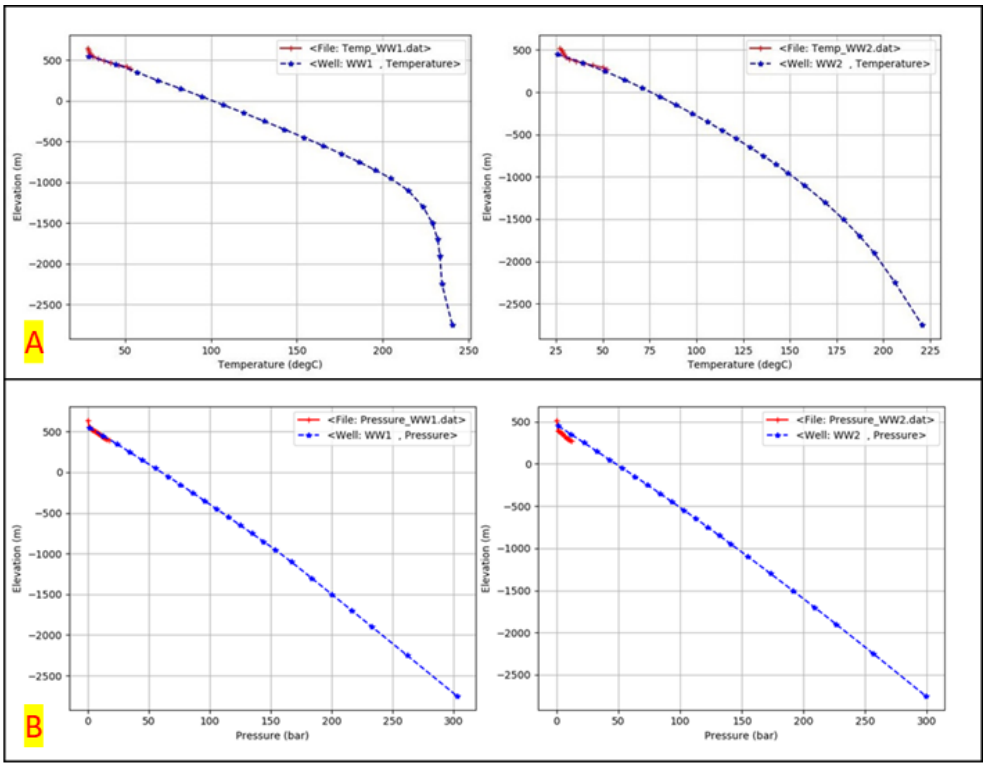

Figure 12: A. Final temperature vs depth plots, B. Final pressure vs depth plots (red: actual data; blue: simulation result)

Geochemical geothermometer: The average reservoir temperature using geochemical geothermometer is estimated to be 230^{0}C. The mass flow in the final model was distributed over several locations and ranges from 4 to 6 kg/s. The temperature of the upflow zone fits with the geothermometer prediction, as the result of the input of 36 kg/s of hot water with the enthalpy of 1,100 kJ/kg assigned into six blocks. The majority of the mass flow is assigned to the Poco Dedeng fault where there is upflow beneath Lake Sano Nggoang. The rest of the mass flow is assigned to Lempe and Nampar fault to facilitate the expected outflow.

Surface manifestation: The available manifestation data only gives a minor discharge from 0.1 from 0.5 l/s, which is equal to 0.1 kg to 0.5 kg/s (Hadi et al., 2015). It is not comparable to the source input at 36 kg/s. High discharge is believed to be occurring beneath Lake Sano Nggoang, thus it is difficult to quantify the volume. As well as acid hot springs, a fumarole is also thought to be beneath the lake. Those assumptions make a good argument for the acid water found all over the lake with a pH value of 2.52. The simulation results are displayed from Figure 13 to Figure 15. They reasonably match with the observed locations of surface manifestations. A fault is expected to be the permeability control that allows upflow beneath Lake Sano Nggoang.

12. ANALYSIS OF NATURAL STATE CALIBRATION

In Well WW1, the temperature profile shows more convection effects compared to the profile for Well WW2. In Well WW2, the temperature profile does not wholly show the linear conduction effect. It is slightly influenced by a convection effect as it is located near Well WW1. WW1 is located near the edge of the reservoir, whereas WW2 is outside the reservoir. In the simulation, the temperature at the top of the reservoir is approximately 200˚C. The temperature will be higher with increasing depth, and it may reach more than 250˚C at 3000 mbsl. Assuming the system contains 100% liquid, the enthalpy of 1100 kJ/kg means the temperature is about 250˚C (Zarrouk & Watson, 2010). A total mass upflow of 36 kg/s with that enthalpy is reasonable, considering the relatively low expected potential power of 36 MWe from the stored heat calculation method (Direktorat Panas Bumi, 2017).

Meanwhile, the model pressure in Well WW2 is still about 6 bars different compared to the actual data. The actual data shows that the water table lies at 120 m below the surface, while the simulation shows it at 70 m below the surface. In WW1, the pressure from the actual and simulation data indicates the same water table at 70 m below the surface. This is a good result as WW1 is adjacent to Lake Sano Nggoang. The distance between WW1 and WW2 is approximately 300 m, and the elevation difference is about 100 m. This means that the simulation results show almost the same water table level, at 70 m, for both wells. Nevertheless, the model still needs improvement to match the actual pressure profile.

It was stated that Nampar Mancing and Golo Lara warm springs are thought to be connected with Waesano geothermal system, while another hypothesis is that it is uncertain if they are related. The calculated isotherms for the Waesano 3D model, show that it would be difficult for the mass flow to reach the more than 12 km distance to the Nampar Mancing warm spring, although some of the mass flow is input at the base of the Lempe and Nampar Faults. As seen in Figure 14 and Figure 15, the simulation shows that the mass

flow could reach as far as around 6 km. This gives rise to two possibilities: either the model still needs improvement (e.g. rock properties, mass flow) or both warm springs are related to another hydrothermal system.

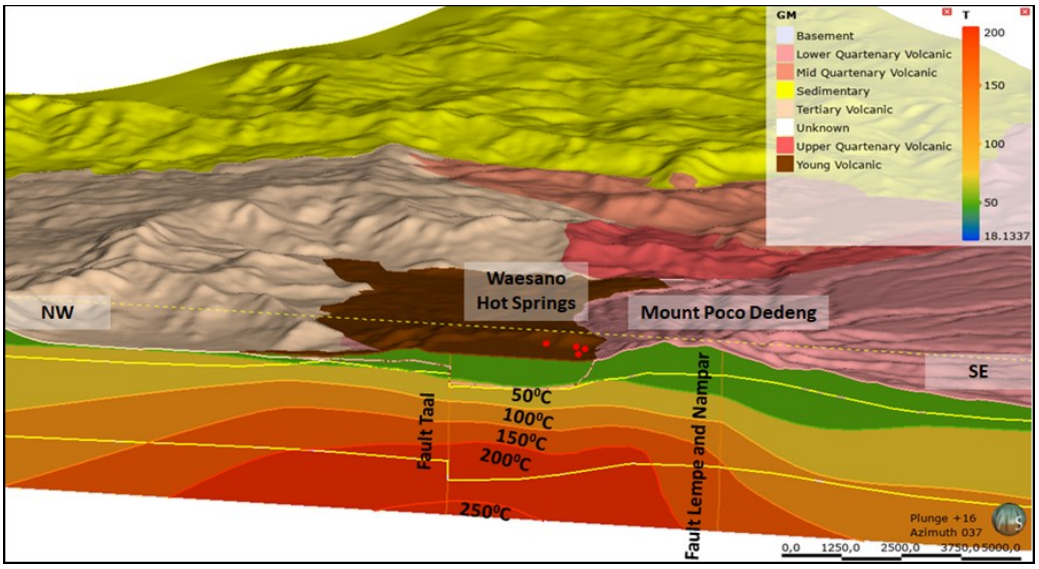

Figure 13: Isotherms in the Waesano 3D Model (parallel with Poco Dedeng Fault)

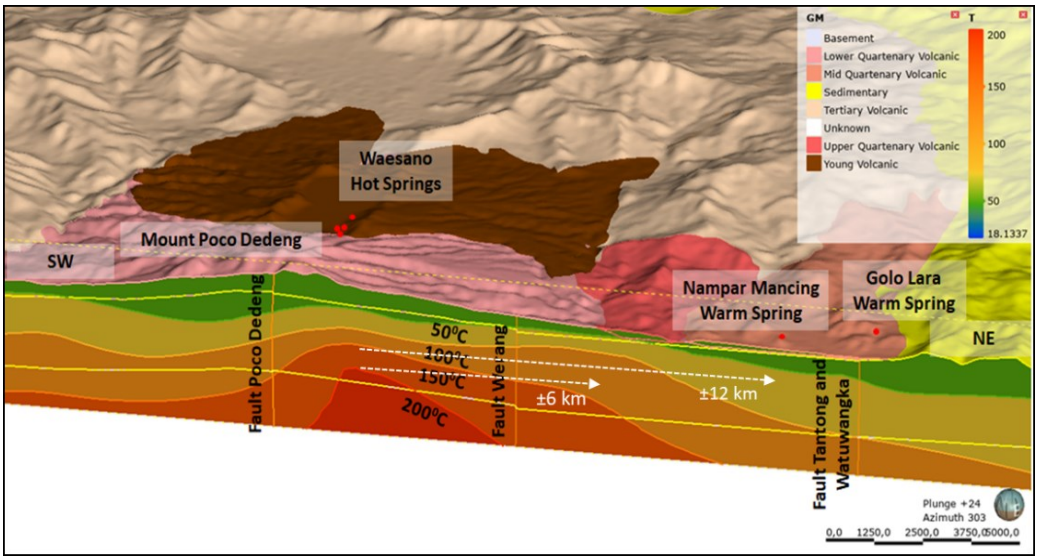

Figure 14: Isotherms in the Waesano 3D Model (parallel with Lempe and Nampar Faults)

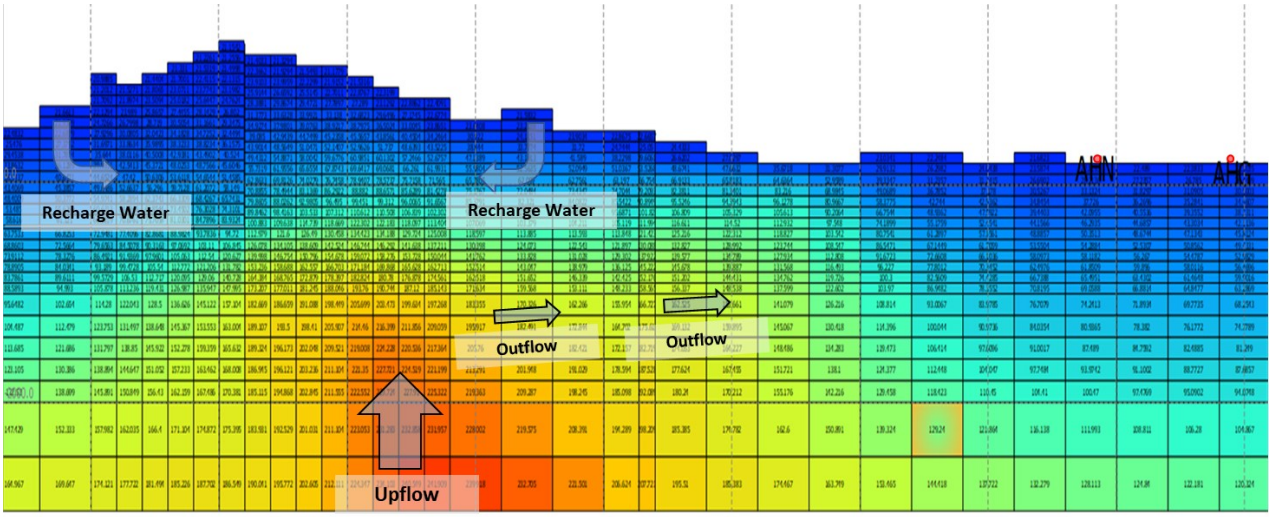

Figure 15. Temperature distribution for the natural state model (parallel with Lempe and Nampar Faults)

13. CONCLUSSION AND RECOMMENDATION

This paper has discussed the building of a new 3D geological model and new natural state model of Waesano geothermal field. The 3D geological model was constructed from available published data using Leapfrog Geothermal software. The 3D geological model was used to convert the geological model in order to build the geometry and input files for the numerical model set-up. The numerical model was then used to generate a natural state model of Waesano geothermal system using the AUTOUGH2 simulator. Manual calibration has resulted in a good match of temperature and pressure profiles from two shallow wells in the area. The results also show reasonable agreement with the geothermometer data from several manifestations. This study may provide useful guidance for the sustainable development and management of the system, especially in the early exploratory stage. As only limited data were utilised in this study, deep exploration well data and a better conceptual model could help to establish an updated and more accurate model. Leapfrog Geothermal can automatically adjust the updated data for the numerical model set-up, thus enhancing the workflow process in both geological modelling and numerical modelling.

Since there were limited data for building the Waesano geological and numerical model, there are a few recommendations for improving the model and for further study, such as: A. Gather more geological data and update the Leapfrog model as they become available, thus creating improved rock assignments in the numerical model; B. Adjust the properties for each rock type to see if there are any substantial differences, since from gravity method, rock density ranges from 2300 kg/m^3 to 2900 kg/m^3; C. Use a finer grid near the surface layer to allow for a better pressure match between the data and model results, thus achieving the correct water table level for Well WW2; D. Simulate future production scenarios after establishing the natural state model. These can assist stakeholders in the next phase of the development of the field.

14. ACKNOWLEDGMENTS

The authors would like to acknowledge the assistance of Seequent for providing the license to use Leapfrog Geothermal

REFERENCES

Badan Geologi. (2019). *Peta Geologi Regional Komodo dan Ruteng, serta Peta Geologi Lembar Gili Motang, Kenari, Nangallili, dan Werang*. Retrieved from https://psg.bgl.esdm.go.id/geomap/

Climate-data.org. (2019). Climate: Wae Sano. Retrieved from https://en.climate-data.org/asia/indonesia/east-nusa-tenggara/wae-sano-562205/

Direktorat Panas Bumi. (2017). *Potensi Panas Bumi Indonesia Jilid 2*. *Jakarta: Direktorat Panas Bumi, Ditjen EBTKE, Kementrian ESDM*.

Google. (2019). Waesano Area. Retrieved from https://www.google.com/map

Hadi, M. N., Kusnadi, D., & Simarmata, R. S. L. (2015). SURVEI GEOLOGI DAN GEOKIMIA PANAS BUMI DAERAH WAESANO, KABUPATEN MANGGARAI BARAT, PROVINSI NUSA TENGGARA TIMUR.

Hochstein, M. P. (2010). Geothermal Prospects of the Eastern Banda Arc Islands (Indonesia). *Proceedings World Geothermal Congress*, (April 2010). Retrieved from http://www.geothermal-energy.org/pdf/IGAstandard/WGC/2010/1115.pdf

Indonesia-tourism.com. (2019). Sano Nggoang Crater Lake. Retrieved from http://www.indonesia-tourism.com/east-nusa-tenggara/sano_nggoang.html

Johnstone, R. D. (2005). Contrasting Geothermal Fields Along the Magmatic Banda Arc, Nusa Tenggara, Indonesia. *World Geothermal Congress 2005*, (April), 24–29.

Kholid, M., Takodama, I., & Nurdin, N. M. (2015). SURVEI TERPADU GAYA BERAT DAN AUDIO MAGNETOTELURIC (AMT) DAERAH PANAS BUMI WAESANO, KABUPATEN MANGGARAI BARAT PROVINSI NUSA TENGGARA TIMUR.

Kholid, M., & Widodo, S. (2015). SURVEI MAGNETOTELURIK (MT) DAN TIME DOMAIN ELEKTROMAGNETIC (TDEM) DAERAH PANAS BUMI WAESANO, KABUPATEN MANGGARAI BARAT PROVINSI NUSA TENGGARA TIMUR.

Nanlohi, F., & Boegis, Z. (2003). Geologi Bawah Permukaan Sumur Ww-1 Lapangan Panas Bumi Waisano – Werang Manggarai Barat , Nusa Tenggara Timur, 1–7. Retrieved from https://psg.bgl.esdm.go.id/geomap/

Pambudi, N. A. (2018). Geothermal power generation in Indonesia, a country within the ring of fire: Current status, future development and policy. *Renewable and Sustainable Energy Reviews*, *81*(March 2017), 2893–2901. https://doi.org/10.1016/j.rser.2017.06.096

Pruess, K., Oldenburg, C. M., & Moridis, G. J. (1998). Overview of TOUGH2, Version 2.0. *TOUGH Workshop 1998*. Retrieved from http://esd.lbl.gov/TOUGHPLUS/proceedings/1998/PruessOldenburgMoridis.pdf

Pusat Sumber Daya Geologi. (2003). Laporan survei Landaian Suhu Sumur WW-2 Lapangan Panas Bumi Waisano-Werang Kabupaten Manggarai Barat Nusa Tenggara Timur. Retrieved from http://psdg.bgl.esdm.go.id/perpus/index.php?p=show_detail&id=641

Zarrouk, S., & Watson, A. (2010). Saturated Steam and Water. Retrieved from https://www.researchgate.net/profile/Sadiq_Zarrouk/publication/269465547_Thermodynamic_and_transport_properties_of_Saturated_Steam_and_Water/data/548cc5590cf214269f20e2b2/Zarrouk-and-Watson-2010.pdf